Pownall, H. J., Pao, Q., Hickson, D., Sparrow, J. T., Kusserow, S. K., & Massey, J. B. (1981) *Biochemistry 20*, 6630.
Schiffer, M., & Edmundson, A. B. (1967) *Biophys. J. 7*, 121.
Segrest, J. P. (1977) *Chem. Phys. Lipids 18*, 7.
Segrest, J. P., & Feldmann, R. J. (1977) *Biopolymers 16*, 2053.
Segrest, J. P., Jackson, R. L., Morrisett, J. D., & Gotto, A. M., Jr. (1974) *FEBS Lett. 38*, 247.
Segrest, J. P., Pownall, H. J., Jackson, R. L., Glenner, G. G., & Pollack, P. S. (1976) *Biochemistry 15*, 3187.
Sober, H. A. (1970) *CRC Handbook of Biochemistry: Selected Data for Molecular Biology*, Second ed., pp B-74–B-76, Chemical Rubber Publishing Co., Cleveland, OH.
Tall, A. R., Small, D. M., Deckelbaum, R. J., & Shipley, G. G. (1977) *J. Biol. Chem. 252*, 4701.
Taylor, J. W., Miller, R. J., & Kaiser, E. T. (1983) *J. Biol. Chem. 258*, 4464.
Terwilliger, T., Weissman, L., & Eisenberg, D. (1982) *Biophys. J. 37*, 353.
Vournakis, J. N., Yan, J. F., & Scheraga, H. A. (1968) *Biopolymers 6*, 1531.
Watts, A., Volotovski, I. D., & Marsh, D. (1979) *Biochemistry 18*, 5006.
Wu, C.-S. C., Lee, N. M., Loh, H. H., Yang, J. T., & Li, C. H. (1979) *Proc. Natl. Acad. Sci. U.S.A. 76*, 3656.
Wu, C.-S. C., Lee, N. M., Ling, N., Chang, J. K., Loh, H. H., & Yang, J. T. (1981a) *Mol. Pharmacol. 19*, 302.
Wu, C.-S. C., Ikeda, K., & Yang, J. T. (1981b) *Biochemistry 20*, 566.

Dependence of Phosphatidylcholine Phosphorus-31 Relaxation Times and $^{31}P\{^1H\}$ Nuclear Overhauser Effect Distribution on Aggregate Structure†

R. A. Burns, Jr., R. E. Stark, D. A. Vidusek, and M. F. Roberts*

ABSTRACT: Phosphorus-31 nuclear magnetic resonance (^{31}P NMR) relaxation rates and $^{31}P\{^1H\}$ nuclear Overhauser effects (NOEs) have been obtained for a variety of phosphatidylcholine monomers, micelles, and sonicated vesicles. NOE measurements conducted with broad-band irradiation of the entire ^1H spectrum monitor the influence of aggregation state on both the overall time scale of molecular motions and the relative contributions of various spin-relaxation pathways. Selective NOE studies are in part consistent with earlier findings [Yeagle, P. L., Hutton, W. C., Huang, C.-H., & Martin, R. B. (1977) *Biochemistry 16*, 4344], which attributed enhanced ^{31}P signal intensity to *N*-methyl protons of the choline head group. In the present lecithin systems, the maximum NOE occurs when methylenes adjacent to the phosphate moiety are irradiated (monomeric lecithin or small nearly spherical micelles) or, in some cases, at a frequency intermediate between these methylenes and the choline methyl group (sonicated egg lecithin vesicles and large micellar species such as those formed by 1,2-dioctanoylphosphatidylcholine). With addition of cholesterol to vesicles or 1,2-dioctanoylphosphatidylcholine micelles, the position of the NOE maximum shifts further away from the choline methyl frequency. For model compounds in which an *N*-methyl group is covalently linked to phosphorus, substantial NOEs from these protons are observed, but contributions from other adjacent methylene protons are also important. Multiple sources of $^{31}P\{^1H\}$ NOEs in these model studies, as well as possible complications from proton cross relaxation in larger aggregates, result in serious ambiguities if such measurements are used to study intermolecular phospholipid head group interactions.

Phosphorus-31 nuclear magnetic resonance (NMR)[1] spectroscopy has been widely used in studies of the conformation and dynamics of phospholipid head groups. The spectral line shape has proven to be a powerful structural probe in partially ordered model-membrane systems (Browning, 1981), and valuable molecular information has been obtained in the solution state from ^{31}P spin-relaxation times (T_1's) and nuclear Overhauser effects (NOEs) (Yeagle, 1978; Yeagle et al., 1977; Moore et al., 1977; Castellino & Violand, 1979). If the entire ^1H spectrum is irradiated, the resulting enhancement in ^{31}P signal intensity allows separation of dipole–dipole (DD) contributions from other relaxation pathways (Noggle & Schirmer, 1971), so that overall relaxation rates may be interpreted in terms of the motional dynamics of the lipid head group (Viti & Minetti, 1981). If ^1H irradiation is applied at frequencies that correspond to single chemical groupings, then selective $^{31}P\{^1H\}$ NOEs are obtained. Since the magnitude of the enhancement depends inversely on the sixth power of the internuclear separation (r^{-6}_{PH}), experiments of this sort provide in principle a nonperturbing probe of phospholipid head group interactions in the solution state (Yeagle, 1978; Viti & Minetti, 1981).

For phosphatidylcholine and sphingomyelin bilayers, Yeagle et al. (1977) reported a $^{31}P\{^1H\}$ NOE profile with a maximum

† From the Department of Chemistry, Massachusetts Institute of Technology, Cambridge, Massachusetts 02139 (R.A.B., D.A.V., and M.F.R.), and the Department of Chemistry, Amherst College, Amherst, Massachusetts 01002 (R.E.S.). *Received March 3, 1983.* This work was supported by grants from the National Science Foundation (PCM-7912622) and the National Institutes of Health (BRSG S074407110). NMR experiments performed at the National Magnet Laboratory were supported by the National Institutes of Health (RR 00995) and the National Science Foundation (C-670).

[1] Abbreviations: NMR, nuclear magnetic resonance; T_1, spin–lattice relaxation time; NOE, nuclear Overhauser effect; 1,2-diacyl-PC or 1,2-diacylphosphatidylcholine, 1,2-diacyl-*sn*-glycero-3-phosphocholine; DD, dipole–dipole spin relaxation; CSA, chemical shift anisotropy relaxation; TLC, thin-layer chromatography; rf, radio frequency; Tris, tris(hydroxymethyl)aminomethane; EDTA, ethylenediaminetetraacetic acid.

0006-2960/83/0422-5084$01.50/0 © 1983 American Chemical Society

at the choline methyl ^1H frequency. This was attributed to an interfacial structure in which lecithin head groups, parallel to the bilayer plane, show intermolecular interactions between a cationic choline and the anionic phosphate of an adjacent lipid molecule. Addition of cholesterol apparently disrupted the interactions, causing the NOE maximum to shift toward ^1H frequencies of methylene groups on either side of the phosphate (Yeagle et al., 1977).

These head group interactions are consistent with the basic bilayer structure detailed by other techniques. A variety of NMR (Seelig & Gally, 1976; Seelig et al., 1977) and diffraction studies (Buldt et al., 1978; Pearson & Pascher, 1979) demonstrate that phosphatidylcholine and phosphatidylethanolamine head groups are oriented parallel to the bilayer plane, though they fail to provide evidence for interaction between oppositely charged moieties. X-ray diffraction work on an anhydrous crystal of 1,2-dilauroyl-DL-phosphatidylethanolamine (Elder et al., 1977) *does* support an intermolecular interaction between ammonium and surrounding phosphate moieties through a 2.8-Å H bond. However, this hydrogen-bonding interaction may not occur in the presence of excess water: an X-ray crystal structure of 1,2-dimyristoyl-PC dihydrate (Pearson & Pascher, 1979) shows the nitrogen atom of the choline moiety approaching no closer than 4.5 Å to phosphate oxygens. Instead of close contact between charged groups, water molecules form a hydrogen-bonded network between adjacent phosphate groups in this crystal. While most studies find the polar head groups oriented parallel to the bilayer plane, evidence for general intermolecular charge interactions comes entirely from the anhydrous X-ray crystal structure and the $^{31}P\{^1H\}$ NOE studies.

This study reports ^{31}P relaxation data and the ^1H frequency dependence of ^{31}P NOEs for phosphatidylcholines in monomer, micelle, and vesicle forms. From measurements of T_1's and nonselective NOEs at two magnetic field strengths, both relative *and* absolute relaxation contributions are determined for DD and chemical shift anisotropy (CSA) pathways (Lyerla & Levy, 1974). These relaxation rates are then examined as a function of lecithin aggregation state. The results may be accounted for solely by changes in the effective tumbling time of the relevant lecithin species, without invoking specific intermolecular head group interactions. Selective $^{31}P\{^1H\}$ NOE experiments yield profiles whose width depends on the size of the lecithin aggregate. The frequency of maximum enhancement corresponds to methylene protons adjacent to the phosphate moiety, for small particles, or for larger aggregates at a frequency intermediate between these methylenes and the choline methyl groups. In the large lecithin micelles, the maximum in the phospholipid NOE profile does shift slightly toward the methylene groups in the presence of cholesterol, in agreement with the findings of Yeagle et al. (1977). If higher proton-decoupling power is used, the NOE profile broadens, and the apparent maximum shifts toward the choline methyl. These ^{31}P NMR studies weakly support the earlier conclusions of Yeagle et al. (1977).

NOE measurements have also been conducted for the model compounds 2-ethoxy-3-methyl-1,3,2-oxazaphospholidine and the oxidized derivative 2-ethoxy-3-methyl-1,3,2λ^5-oxazaphospholidin-2-one, each of which has an *N*-methyl group covalently bonded to phosphorus. Our results demonstrate that for monomeric compounds the methyl protons can contribute substantially to the observed NOE when separated by two covalent bonds from the phosphorus of the phosphoramidate moiety. But even with a methyl proton that can approach as close as *2.3* Å from the phosphorus, both ring and side-chain methylenes also influence the observed $^{31}P\{^1H\}$ NOE profile. Measurements on these model compounds and the results for several well-studied mixed micellar particles suggest that for micellar aggregates the width of the NOE distribution is a more reliable monitor of lecithin head group interactions than the ^1H frequency of the maximum NOE.

Experimental Procedures

Materials. 1,2-Dihexanoyl-PC and 1,2-dibutyryl-PC were obtained from Calbiochem; 1,2-diheptanoyl-PC and 1,2-dioctanoyl-PC were synthesized as described previously (Burns & Roberts, 1980). Phospholipid purity was monitored by TLC (Burns & Roberts, 1980). The preparation of short-chain lecithin mixed micelles with tributyrin and cholesterol has been described previously (Burns & Roberts, 1981a,b). Unilamellar egg phosphatidylcholine (Makor) vesicles were prepared by sonifying (Branson 350 cell disruptor) aqueous lecithin solutions in a water-cooled cell (Wilbur Scientific) under an N_2 atmosphere. Large multilamellar particles were removed by ultracentrifugation (Barenholz et al., 1977).

The model compounds 2-ethoxy-3-methyl-1,3,2-oxazaphospholidine and 2-ethoxy-3-methyl-1,3,2λ^5-oxazaphospholidin-2-one were synthesized by following literature procedures (Mukaiyama & Kodaira, 1966; Kodaira & Mukaiyama, 1966). Selective ^1H and ^{31}P decoupling were used to make proton NMR assignments for these compounds solubilized in CD_2Cl_2 and referenced to internal Me_4Si.

NMR Spectroscopy. ^{31}P NMR spectra at 109.3 MHz were obtained on a Bruker 270 spectrometer equipped with a Nicolet 1080 data system; measurements at 40.5 MHz were made on Varian XL-100 or JEOL FX-100Q spectrometers. Spin–lattice relaxation times (T_1's) and NOEs were determined at 25 °C as described previously (Burns & Roberts, 1980). Selective NOEs (at 40.5 MHz) were obtained with a single-frequency proton irradiation, where the methyl and methylene portions of the ^1H spectrum were sampled (randomly) in 5-Hz increments. The power level was adjusted to decouple the protons of trimethyl phosphate in D_2O within 5 Hz of the observed ^1H frequency. This produces a large signal enhancement but not a very selective ^1H frequency profile (as judged by the width of the NOE distribution). The irradiation power was then set to a level at which peak enhancement was about 75–85% of the maximum value. For example, on the JEOL FX-100Q a power setting of H(igh)-5.5 leads to 10% enhancement, H-6.0 to 40%, and H-6.5 to 46% enhancement of the 1,2-dioctanoyl-PC signal. Although the magnitude of the maximum enhancement is similar for H-6.0 and H-6.5 settings, the $^{31}P\{^1H\}$ NOE profile width doubles with the higher decoupling power. Proton-decoupling power was gated on only during the waiting time (5–10 times ^1H T_1 values) between acquisitions of phosphorus signals.

^{31}P-decoupled ^1H spectra were obtained at 270.133 MHz on a Bruker WM 270 spectrometer controlled by an Aspect 2000 computer (three clock version). The spectrometer was modified as follows: with the broad-band probe (tunable 27–155 MHz) installed in the spectrometer, the coil normally used for proton decoupling was connected to a 270-MHz ^1H bypass filter and then to the proton observe channel of the spectrometer. The ^{31}P decoupling frequency was generated with a Rockland Model 5600 frequency synthesizer. The ^{31}P frequency was then noise modulated (bandwidth approximately 500 Hz at 1 V) and passed to an ENI Corp. rf amplifier where the signal was increased to approximately 1 W. The rf signal was then passed through a stripling attenuator and finally to the broad-band channel of the probe. The broad-band observe coil was tuned for ^{31}P at 109.367 MHz. The spectrometer

Table I: ^{31}P Spin-Lattice Relaxation Times and Nuclear Overhauser Effects in Phosphatidylcholines

phospholipid system	T_1 (40.5 MHz) obsd[a]	T_1 (40.5 MHz) calcd[b]	T_1 (109.5 MHz) obsd	T_1 (109.5 MHz) calcd	NOE (40.5 MHz) obsd	NOE (40.5 MHz) calcd	NOE (109.5 MHz) obsd	NOE (109.5 MHz) calcd
egg PC vesicles	3.1	2.5	1.1	1.4	1.7	1.5	1.2	1.1
1,2-dioctanoyl-PC micelles	3.5	3.0	1.7	2.3	1.8	1.8	1.4	1.2
1,2-diheptanoyl-PC micelles	3.9	3.4	2.0	2.6	1.9	1.8	1.4	1.2
1,2-dihexanoyl-PC micelles	5.4	5.0	2.5	3.1	1.8	1.8	1.4	1.2
1,2-dibutyryl-PC monomers	13	13	6.5	6.5	1.8	2.2	1.4	1.3

[a] Error limits, estimated from repeated measurements, are 10% for T_1's and 15% for NOEs. [b] Parameters are calculated from eq 1-2', by using best fit values for R(DD) and R(CSA).

itself was operating in the normal proton mode with the broad-band ^{31}P decoupling on at all times.

Data Analysis. Nonselective $^{31}P\{^1H\}$ NOEs were analyzed by assuming that spin relaxation occurs via a combination of ^{31}P–^1H dipolar (DD) and ^{31}P chemical shift anisotropy (CSA) interactions:

$$R(\text{total}) = R(\text{DD}) + R(\text{CSA}) \quad (1)$$

where $R(\lambda) \equiv 1/T_1^{\lambda}$ in each case and other possible mechanisms are ignored. Under "extreme narrowing" conditions (molecular tumbling rapid compared with the NMR resonance frequency),[2] the phosphorus NOE is given by (Lyerla & Levy, 1974)

$$\text{NOE} = 1 + \frac{\gamma_H}{\gamma_P}\frac{R(\text{DD})}{R(\text{DD}) + R(\text{CSA})} \quad (2)$$

where γ_i's are magnetogyric ratios for each nucleus. If eq 1 and 2 are taken to apply at 40.5 MHz, then analogous relations hold at 109.3 MHz, except that R(CSA) increases with the square of the magnetic field strength:

$$R'(\text{total}) = R(\text{DD}) + 7.3R(\text{CSA}) \quad (1')$$

and

$$\text{NOE}' = 1 + \frac{\gamma_H}{\gamma_P}\frac{R(\text{DD})}{R(\text{DD}) + 7.3R(\text{CSA})} \quad (2')$$

In practice, experimental values R(total) and R'(total) were inserted in eq 1 and 1' to obtain initial guesses for R(DD) and R(CSA). These relaxation rates were then adjusted to minimize both individual and total deviations from the observables R(total), R'(total), NOE, and NOE'.

Results

Mechanisms for ^{31}P Relaxation of Phospholipids. ^{31}P T_1 and $^{31}P\{^1H\}$ NOE measurements at two field strengths (Table I) provide a quantitative assessment of dipolar and chemical shift anisotropy contributions to the NMR relaxation of phospholipid phosphorus nuclei. If the relaxation process were entirely dipolar, an NOE of 3.24 (i.e., $1 + \gamma_H/\gamma_P$) would be predicted in the extreme narrowing limit. This formalism should be adequate to describe rapidly tumbling lecithin monomers and micelles, so that reduced values (Table I) may be attributed to CSA contributions to the relaxation. Results presented in Table II indicate that the *relative* DD and CSA contributions remain remarkably constant among PC monomer and micelle samples, even though *absolute* relaxation rates (and measured T_1 values) vary dramatically. Large DD and CSA relaxation rates, and correspondingly short observed ^{31}P T_1's, are found for 1,2-dioctanoyl- and 1,2-diheptanoyl-PC micelles, indicating sluggish head group reorientation in the larger aggregates. If intermolecular head group interactions in micellar aggregates brought additional protons close to the choline phosphate group, an enhanced DD contribution to the relaxation might be expected; our data provide no evidence for this hypothesis.

A similar analysis of T_1's and NOEs for egg PC vesicles would indicate a 15% drop in the fraction of DD relaxation, but this conclusion is misleading. Several estimates put the choline tumbling time (τ_c) at $\sim 10^{-9}$ s (Browning, 1981), so that extreme narrowing conditions ($\omega^2\tau_c^2 \ll 1$) are no longer fulfilled under our experimental conditions [$\omega/(2\pi) = 40.5$ and 109.3 MHz]. If eq 2 and 2' are modified to account for

[2] Cases in which this assumption is likely to break down are described under Results.

Table II: Dipole–Dipole and Chemical Shift Anisotropy Relaxation Rates in Phosphatidylcholines

phospholipid system	R(DD)[a]	R(CSA)[a]	% dipolar
1,2-dioctanoyl-PC micelles	0.24	0.05	83
1,2-diheptanoyl-PC micelles	0.22	0.04	85
1,2-dihexanoyl-PC micelles	0.15	0.035	81
1,2-dibutyryl-PC monomers	0.065	0.012	84

[a] Best fit rates of NMR relaxation at 40.5 MHz.

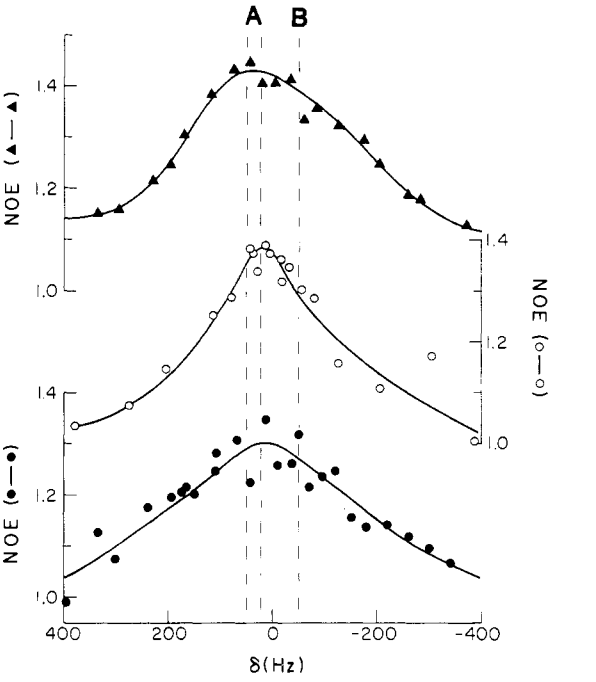

FIGURE 1: ^{31}P NOE as a function of proton decoupling frequency for egg lecithin sonicated vesicles in D_2O. ^1H chemical shifts (δ) are referenced to the methyl protons of external trimethyl phosphate. The dashed lines indicate shifts of methylene groups adjacent to the phosphate moiety (A) and of choline methyl groups (B). The experimental curves describe vesicles in D_2O with 50 mM Tris-HCl buffer, pD 7.4 (▲), vesicles in D_2O alone, pD 7.4 (○), and vesicles in 100 mM NaCl–5 mM EDTA, pD 7.9 (●).

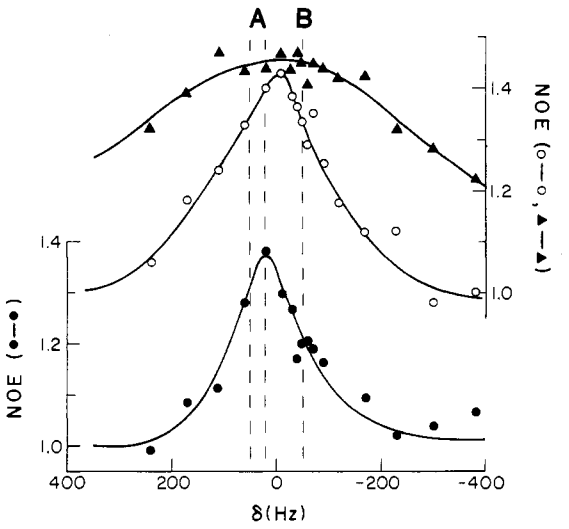

FIGURE 2: ^{31}P NOE as a function of proton decoupling frequency for 1,2-dioctanoyl-PC micelles in D_2O: pure 1,2-dioctanoyl-PC micelles (○); 1,2-dioctanoyl-PC micelles with 15 mol % cholesterol (●); pure 1,2-dioctanoyl-PC micelles with a 4-fold increase in ^1H decoupling power (▲).

slower motions in vesicle systems (London, 1980), then smaller NOE values are predicted even if the ratio $R(DD)/R(CSA)$ remains constant.

$^{31}P\{^1H\}$ NOE Profiles for Lecithins in Different Aggregation States. Figure 1 shows the NOE frequency dependence for egg PC sonicated vesicles prepared under slightly varying experimental conditions (low salt with and without buffer and high salt). Selective proton decoupling reduces the maximum NOE values slightly, and the exact enhancement also depends on the power level of rf irradiation. Nevertheless, all profiles show a maximum at proton frequencies between the methylenes adjacent to the phosphate moiety (frequencies indicated by dashed lines at A) and $N(CH_3)_3$ protons (indicated by dashed line B), in some disagreement with the data of Yeagle et al. (1977). The maxima are clearly *not* centered at the *N*-methyl frequency (B) under any of these conditions.

Several other PC samples give similar results. For 1,2-dioctanoyl-PC micelles, the NOE maximum is again centered between the methylene and choline methyl frequencies (Figure 2, ○). In the presence of 15 mol % cholesterol (close to the maximum amount that can be solubilized by these micelles), the profile does shift further away from the choline methyls (Figure 2, ●) and is biased slightly more toward methylene frequencies. Under these conditions, the trends in the position of the maximum are in accord with previous reports for bilayer systems (Yeagle et al., 1977). However, if the proton decoupling power is increased (on the JEOL FX-100Q from H-6.0 to H-6.5), the NOE distribution becomes significantly broader and appears to show larger contributions at the choline methyl frequency (Figure 2, ▲). Figure 3 shows profiles for 1,2-diheptanoyl-PC in the absence (○) and presence (●) of saturating amounts of tributyrin. The NOE maximum occurs at an intermediate frequency between A and B, perhaps slightly biased toward the methylene groups. Tributyrin does not affect the shape of the NOE or position of the maximum NOE, although the magnitude of the NOE is reduced. Finally, NOE profiles for micellar 1,2-dihexanoyl-PC and monomeric 1,2-dibutyryl-PC (Figure 4) are clearly centered at the phosphate methylenes; in these samples, any NOE contribution from choline methyl protons is considerably smaller than that seen in the bilayer or in larger micellar aggregates.

The widths of the $^{31}P\{^1H\}$ NOE profiles are summarized in Table III. While there is some scatter in the data, the ob-

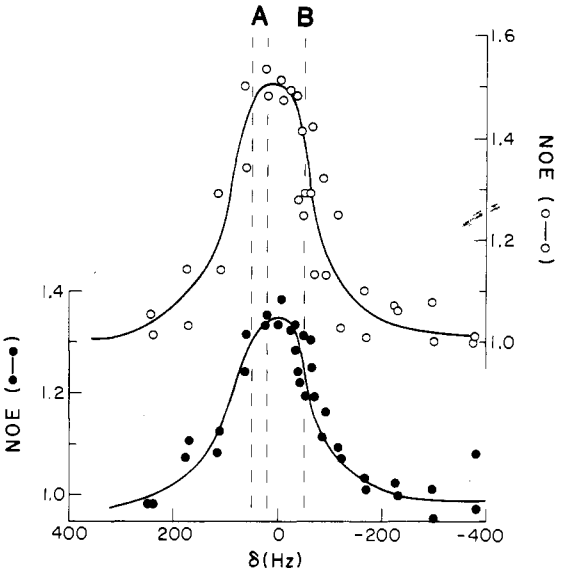

FIGURE 3: ^{31}P NOE as a function of proton decoupling frequency for 1,2-diheptanoyl-PC micelles in D_2O: pure lecithin micelles (○); lecithin with 20 mol % tributyrin (●).

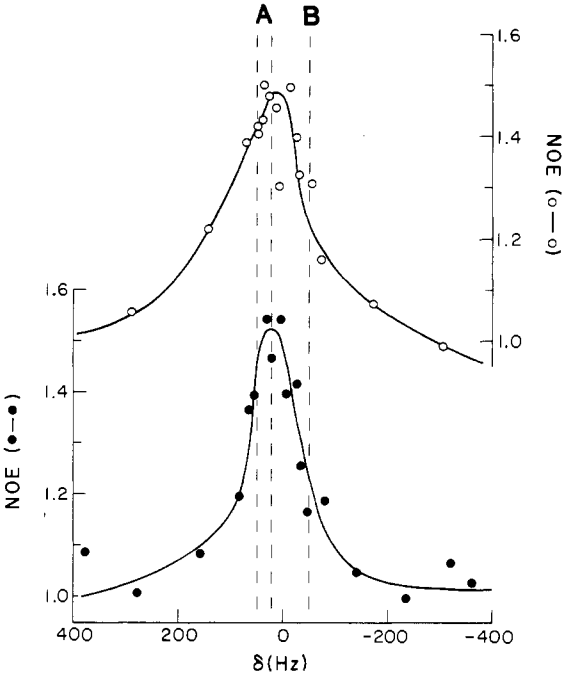

FIGURE 4: ^{31}P NOE as a function of proton decoupling frequency for 1,2-dibutyryl-PC monomers in D_2O (●) and for 1,2-dihexanoyl-PC micelles in D_2O (○).

Table III: Width of Selective $^{31}P\{^1H\}$ NOE Profiles[a]

phospholipid system	profile width (Hz)[b]
egg PC vesicles	370 (80)
1,2-dioctanoyl-PC micelles	200 (25)
1,2-dioctanoyl-PC micelles, cholesterol	160 (15)
1,2-diheptanoyl-PC micelles	160 (10)
1,2-diheptanoyl-PC micelles, tributyrin	160 (15)
1,2-dihexanoyl-PC micelles	170 (10)
monomers[c]	100 (10)

[a] All NOEs measured at a ^1H power level adjusted as described under Experimental Procedures. [b] The width of the distribution at half the peak enhancement; values in parentheses represent standard deviations. [c] 1,2-Dibutyryl-PC, 2-ethoxy-3-methyl-1,3,2-oxazaphospholidine, 2-ethoxy-3-methyl-1,3,2λ⁵-oxazaphospholidin-2-one, and 1,2-dioctanoyl-PC in organic solvents such as CD_3OD.

served widths of the $^{31}P\{^1H\}$ NOE profiles clearly distinguish monomer, micelle, and vesicle species. The widths also appear to reflect the addition of surface-active compounds to the micelles.

$^{31}P\{^1H\}$ NOE Profiles for Model Compounds. A 270-MHz ^1H NMR spectrum of 2-ethoxy-3-methyl-1,3,2-oxazaphospholidine is shown in Figure 5A. Methylene chemical shifts, all downfield of the N–CH_3 resonance, are at 4.13, 3.69, and 3.01 ppm. The resonance centered at 3.01 ppm appears as a complex multiplet with a broad doublet pattern, each wing integrating to one proton. On the basis of chemical shifts and comparison with other CH_2N groups, this pattern can be attributed to the nonequivalent CH_2N protons in the constrained ring system. Selective irradiation of the CH_2N protons perturbs/partially collapses the resonance at 4.13 ppm. Likewise, selective irradiation at 4.13 ppm collapses both proton resonances centered at 3.01 ppm. This experiment assigns the signal at 4.13 ppm to be that of the CH_2 ring protons. Throughout these decoupling experments, the resonance at 3.69 ppm remains unperturbed. Selective irradiation of this resonance similarly does not perturb the signals at 4.13 or 3.01 ppm. This resonance, therefore, has been assigned to the methylene protons of the ethoxy group. The assignment of the other protons is straightforward: the N–CH_3 resonance is a doublet centered at 2.7 ppm with a phosporus coupling constant of 10 Hz, and the methyl of the ethoxy group is found at 1.17 ppm. Resonances coupled to the phosphorus are identified by ^{31}P decoupling (Figure 5B); multiplet peaks at 2.70, 3.01, 3.69, and 4.13 ppm are all partially collapsed. Thus, all protons two bonds from the phosphorus atom show scalar coupling to that nucleus. The $^{31}P\{^1H\}$ NOE profile for this compound is shown in Figure 6A. This model compound, where the NCH_3 moiety is covalently linked to the phosphorus, shows the NOE optimum much closer to the NCH_3 protons (in fact, nearly centered on the CH_2N protons) than to the CH_2OP moieties. This behavior is in marked contrast to that of lecithin aggregates.

A similar NOE profile is observed for 2-ethoxy-3-methyl-1,3,2λ^5-oxaphospholidin-2-one (Figure 6B). Once again, the profile is biased more toward the NCH_3 protons than that in lecithin systems (almost centered on the CH_2N). It is also a narrow profile consistent with monomeric structures.

Discussion

Does the $^{31}P\{^1H\}$ NOE Monitor Intermolecular Phospholipid Head Group Interactions? These studies of vesicle and large micellar phospholipid systems show a maximum in the $^{31}P\{^1H\}$ NOE frequency profile at a position intermediate between the phosphate methylene and *N*-methyl proton positions. Monomers and small spherical micelles show narrower distributions that are clearly centered at the methylene frequencies. Larger micelles and vesicles show progressively broader distributions, with the maximum of the distribution shifting to a frequency intermediate between methylene and choline methyl resonances. None of the lecithins studied displays a profile with a clear maximum at the choline methyl frequency, as reported previously (Yeagle et al., 1977; Moore et al., 1977; Viti & Minetti, 1981).

One possible explanation for this discrepancy is the use of too high a decoupling power in the earlier studies, leading to distortions such as those illustrated in Figure 2. In light of the proximity of methylene and choline methyl resonances (70- and 100-Hz separation at 2.3 T) and the breadth of the NOE distributions (up to 350 Hz), instrumental limitations make this technique less than ideal for investigation of proposed intermolecular head group interactions. Even for model compounds with NCH_3 protons as close as 2.3 Å (based on simple geometry arguments) to the phosphorus nucleus, interpretation of the NOE data is complicated by contributions from other molecular moieties. Thus even in a system where head group interactions occur, it would be difficult to measure them unambiguously via NOE contributions from a single type of proton grouping.

An additional caveat should be noted regarding the use of selective $^{31}P\{^1H\}$ NOEs to investigate proximity between the head group phosphate and protons at particular molecular sites. If aggregate tumbling is slow and the phospholipid protons form a rigid "spin reservoir", then dipolar cross relaxation among the protons (Bothner-By, 1979) may compete effectively with ^1H–^{31}P dipole–dipole interactions. The predominance of ^{31}P NOE contributions from nearby protons would be diminished, resulting in a broadened NOE profile that reflects proton spin diffusion as well as distance-dependent proton–phosphorus interactions. In fact, as noted above (Table III), the width of the NOE profile increases as the particle size grows from monomer to micelle vesicle. The increase in profile width is most pronounced for vesicle structures where aggregate tumbling would be the slowest. Moreover, proton cross relaxation has been observed independently by two-dimensional NOE techniques for motionally restricted regions of long-chain phospholipids solubilized in bile salt detergent micelles (R. E. Stark and M. F. Roberts, unpublished results) so that proton cross relaxation is potentially a problem in large aggregates.

Even with these limitations, the $^{31}P\{^1H\}$ NOE frequency dependence profile shows some sensitivity to size and surface composition of mixed micelles. 1,2-Dioctanoyl-PC forms large micelles, and of all the pure lecithin micelle systems, it appears to have the largest NOE contribution from the *N*-methyl protons. We have shown previously that 15 mol % cholesterol can be solubilized with this lipid (Burns & Roberts, 1981b); ^{13}C NMR evidence suggests that the cholesterol hydroxyl group and part of ring A are at the interface. If so, cholesterol would be expected to affect lecithin intermolecular head group interactions. If the cholesterol hydroxyl group were interacting strongly with the phosphate, then the C(3)–H (and possibly other ring protons) might be expected to enhance the dipolar relaxation (and hence NOE) of the phosphorus nucleus. If the cholesterol hydroxyl is in close proximity to the fatty acyl carbonyls, however, then lecithin head group associations would be disrupted so that the $^{31}P\{^1H\}$ NOE would decrease. In fact, a saturating level of cholesterol decreases the maximum NOE value slightly and also shifts the maximum of the $^{31}P\{^1H\}$ NOE profile noticeably toward the CH_2OP region. The incorporation of cholesterol also increases the aggregate radius by ~50% (R. A. Burns, Jr., and M. F. Roberts, unpublished results) and enhances the proportion of lecithin-chain trans conformers (Burns & Roberts, 1981b). Thus, addition of cholesterol would produce a broadening of the NOE profile if proton cross relaxation were important in this system. Instead, the profile width decreases, and the altered maximum may be interpreted in terms of changes in head group interactions.

Tributyrin can also be solubilized in the lecithin micelles (Burns & Roberts, 1981a). The addition of 20 mol % tributyrin to 1,2-diheptanoyl-PC micelles causes considerable particle shrinkage: from about 60 to 35 Å. The small, spherical particles produced have 5–10% of the saturating tributyrin at the surface (a maximum of 0.33 mol fraction tributyrin can be solubilized by 1,2-diheptanoyl-PC) (Burns et al., 1983). In such a particle, it is plausible that the tri-

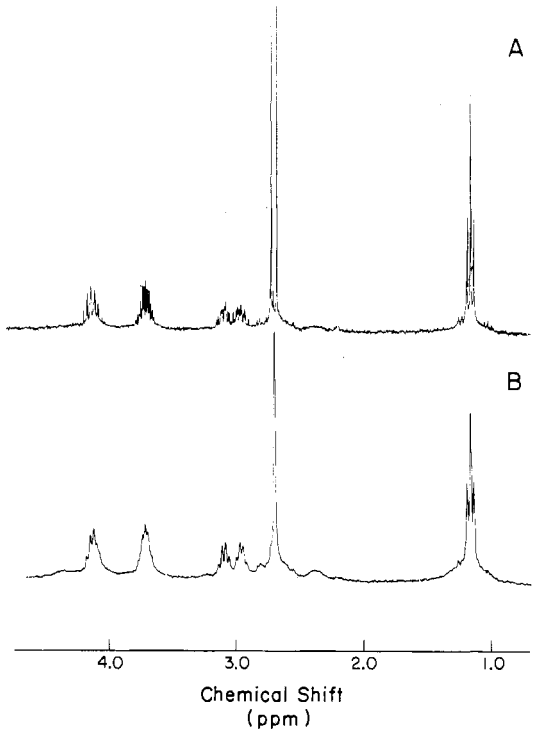

FIGURE 5: (A) ^{1}H NMR spectrum of model compound 2-ethoxy-3-methyl-1,3,2-oxazaphospholidine; (B) ^{31}P-decoupled ^{1}H NMR spectrum of 2-ethoxy-3-methyl-1,3,2-oxazaphospholidine.

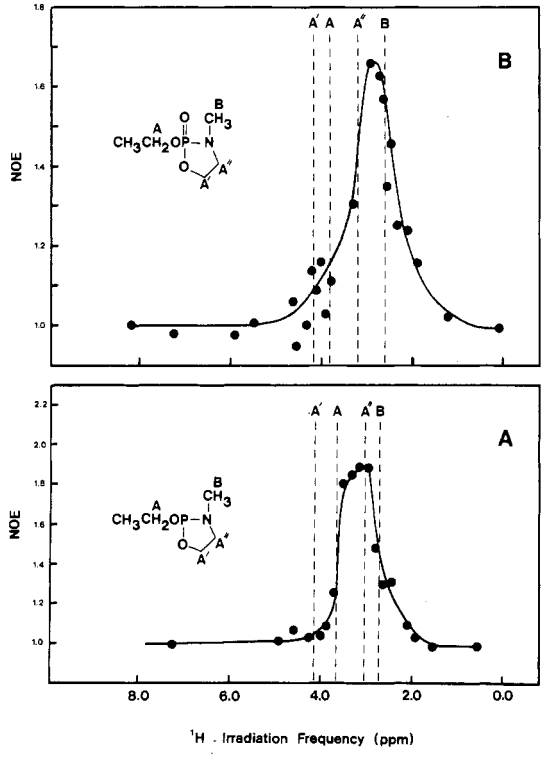

FIGURE 6: ^{31}P NOE as a function of proton decoupling frequency for model compounds in CD_2Cl_2: (A) 2-ethoxy-3-methyl-1,3,2-oxazaphospholidine; (B) 2-ethoxy-3-methyl-1,3,2λ^5-oxazaphospholidin-2-one. The dashed lines indicate specific proton chemical shifts identified by chemical group.

butyrin does not disrupt lecithin head group interactions to a large extent. This is, in fact, observed—the width of the $^{31}P\{^{1}H\}$ NOE distribution and the ^{1}H frequency of the maximum NOE are unaltered. (Again, the lack of change in the NOE profile with dramatic changes in particle size suggests that proton cross relaxation is not biasing the expeiment.) However, different physical studies (Burns et al., 1983) have shown that subsaturating amounts of tributyrin preferentially partition to the surface rather than to the core of the mixed particle. The data in Figure 3 are for 0.20 mol fraction tributyrin in 1,2-diheptanoyl-PC. At most, one out of five triglyceride molecules would be at the surface. While $^{31}P\{^{1}H\}$ NOE data yield no hint of this surface pool, ^{31}P line widths are sensitive to this surface tributyrin (Burns et al., 1983). While the interpretation of these data in terms of dipolar interactions with nearby protons provides a geometric picture consistent with previous investigations of these two mixed particles, the $^{31}P\{^{1}H\}$ NOE technique fails to provide direct or unambiguous information on the surface structure of phospholipid aggregates. Difficulties in probing head group interactions will be enhanced in larger vesicle structures. In summary, the usefulness of $^{31}P\{^{1}H\}$ NOEs appears quite limited for defining lecithin head group interactions in poorly characterized aggregate systems.

Acknowledgments

We thank Larry Coury for synthesis of 2-ethoxy-3-methyl-1,3,2-oxazaphospholidine. We also thank a referee for suggesting the possibility of proton cross relaxation in these aggregate systems.

Registry No. 1,2-Dioctanoyl-PC, 19191-91-4; 1,2-diheptanoyl-PC, 39036-04-9; 1,2-dihexanoyl-PC, 34506-67-7; 1,2-dibutyryl-PC, 3355-26-8; 2-ethoxy-3-methyl-1,3,2-oxazaphospholidine, 7077-42-1; 2-ethoxy-3-methyl-1,3,2λ^5-oxazaphospholidin-2-one, 7010-06-2; cholesterol, 57-88-5; tributyrin, 60-01-5.

References

Barenholz, Y., Gibbes, D., Litman, B. J., Goll, J., Thompson, T. E., & Carlson, F. D. (1977) *Biochemistry 16*, 2806.

Bothner-By, A. A. (1979) in *Biological Applications of Magnetic Resonance* (Shulman, R. G., Ed.) pp 177–219, Academic Press, New York.

Browning, J. L. (1981) in *Liposomes: From Physical Structure to Therapeutic Applications* (Knight, C. G., Ed.) pp 189–242, Elsevier/North-Holland, Amsterdam.

Buldt, G., Gally, H.-U., Seelig, A., Seelig, J., & Zaccai, G. (1978) *Nature (London) 271*, 182.

Burns, R. A., Jr., & Roberts, M. F. (1980) *Biochemistry 19*, 3100.

Burns, R. A., Jr., & Roberts, M. F. (1981a) *J. Biol. Chem. 256*, 2716.

Burns, R. A., Jr., & Roberts, M. F. (1981b) *Biochemistry 20*, 7102.

Burns, R. A., Jr., Donovan, J. M., & Roberts, M. F. (1983) *Biochemistry 22*, 964.

Castellino, F. J., & Violand, B. N. (1979) *Arch. Biochem. Biophys. 193*, 543.

Elder, M., Hitchcock, P., Mason, R., & Shipley, G. G. (1977) *Proc. R. Soc. London, Ser. A 354*, 157.

Kodaira, Y., & Mukaiyama, T. (1966) *J. Org. Chem. 31*, 2903.

London, R. E., (1980) in *Magnetic Resonance in Biology* (Cohen, J. S., Ed.) Vol. 1, pp 1–69, Wiley-Interscience, New York.

Lyerla, J. R., Jr., & Levy, G. C. (1974) *Top. Carbon-13 NMR Spectrosc. 1*, 81.

Moore, N. F., Patzer, E. J., Wagner, R. R., Yeagle, P. L., Hutton, W. C., & Martin, R. B. (1977) *Biochim. Biophys. Acta 464*, 234.

Mukaiyama, T., & Kodaira, Y. (1966) *Bull. Chem. Soc. Jpn. 39*, 1297.

Noggle, J. H., & Schirmer, R. E. (1971) *The Nuclear Ov-*

erhauser Effect, Academic Press, New York.
Pearson, R. H., & Pascher, I. (1979) *Nature (London) 281*, 499.
Seelig, J., & Gally, H.-U. (1976) *Biochemistry 15*, 5199.
Seelig, J., Gally, H.-U., & Wohlgemuth, R. (1977) *Biochim. Biophys. Acta 467*, 109.
Viti, V., & Minetti, M. (1981) *Chem. Phys. Lipids 28*, 215.
Yeagle, P. L. (1978) *Acc. Chem. Res. 11*, 321.
Yeagle, P. L., Hutton, W. C., Huang, C.-H., & Martin, R. B. (1977) *Biochemistry 16*, 4344.

Activation of Yeast Pyruvate Carboxylase: Interactions between Acyl Coenzyme A Compounds, Aspartate, and Substrates of the Reaction†

Dorothea E. Myers,* Bernadine Tolbert, and Merton F. Utter

ABSTRACT: Chicken liver pyruvate carboxylase has an absolute requirement for short-chain acyl coenzyme A (CoA), whereas the same enzyme from yeast has less stringent requirements. The yeast enzyme has now been studied in an effort to elucidate the mechanism by which acyl-CoA stimulates pyruvate carboxylase activity. Yeast pyruvate carboxylase has an apparent basal level of activity above which CoA and acyl-CoAs of 2–20 carbons activate; the concentration of acyl-CoA required for half-maximum activation ($K_{0.5}$) decreases as the chain length of the acyl moiety increases to 16 carbons. Activation of yeast pyruvate carboxylase by acyl-CoA is brought about in part by increasing the affinity of pyruvate carboxylase for two substrates, bicarbonate and pyruvate. The affinity of pyruvate carboxylase for bicarbonate is also increased by potassium ions. The observation of only low levels of activity in the absence of acyl-CoA or potassium ion leads to the conclusion that the basal activity so frequently referred to is probably due to the presence of activating monovalent cations. Pyruvate carboxylase from yeast probably has an absolute requirement for monovalent cations or acyl-CoA with a combination of the two being required for optimum conditions for maximal activity. Stimulation by acyl-CoA and inhibition by aspartate are mutually antagonistic with each affecting the activation or inhibition constant and the degree of cooperativity brought about by the other. The enzyme from liver is unaffected by aspartate.

Pyruvate carboxylase [pyruvate:CO_2 ligase (ADP), EC 6.4.1.1], first isolated from avian liver by Utter & Keech (1963), catalyzes the direct carboxylation of pyruvate to oxalacetate according to the following reaction:

$$\text{pyruvate} + MgATP^{2-} + HCO_3^- \xrightarrow[\text{(acyl-CoA)}]{M^+,\ M^{2+}} \text{oxalacetate} + MgADP^- + P_i^{2-}$$

This enzyme has an anaplerotic function, replacing TCA cycle intermediates, as well as being implicated in glycerogenesis in addition to gluconeogenesis from three-carbon compounds. Several pyruvate carboxylases from different sources have been described and their properties reviewed by Utter et al. (1975). Their activities are not affected in the same way by acyl-CoA[1] compounds. The avian liver enzyme, as well as that from *Bacillus licheniformis*, absolutely requires acetyl-CoA (Utter & Keech, 1963; Renner & Bernlohr, 1972); the enzymes from photosynthetic bacteria (Fuller et al., 1961), *Arthrobacter globiformis* (Gurr & Jones, 1977), a thermophilic bacillus (Libor et al., 1978), rat liver (Henning & Seubert, 1964) and bakers' yeast (Ruiź-Amil et al., 1965; Cooper & Benedict, 1966) are activated by acetyl-CoA; the enzymes from *Aspergillus niger* (Bloom & Johnson, 1962) and *Pseudomonas citronellolis* (Seubert & Remberger, 1961) are not affected by acetyl-CoA. Except for the inducible pyruvate carboxylases from *P. citronellolis* and *Azotobacter vinelandii* (Scrutton & Taylor, 1974), all these enzymes have been characterized as large proteins of M_r ~500 000 and are composed of four apparently identical polypeptide chains. Electron microscopy has revealed that the quaternary structure is that of a rhombus (Cohen et al., 1979; Valentine, 1968). The enzymes that have been studied in detail show a striking degree of resemblance with respect to the properties of the catalytic site such as metal ion specificity, nucleotide specificity, presence of biotinyl residues, and, in most instances, apparent K_m values for all three substrates. Further, although modification of the nucleotide portion of the acyl-CoA molecule causes loss of the allosteric activation potential in all cases so far examined, the enzymes exhibit unique patterns of specificity for activation by acyl analogues of acetyl-CoA (Fung, 1972; Tolbert, 1970; Scrutton, 1974).

Phosphoenolpyruvate carboxylases from *Salmonella typhimurium* (Theodore & Englesberg, 1964) and *Escherichia coli* (Amarasingham, 1959; Ashworth et al., 1965) have a function equivalent to that of pyruvate carboxylase in the synthesis of oxalacetate and are also activated by acetyl-CoA (Cañovas & Kornberg, 1965; Maeba & Sanwal, 1965). The inhibition of phosphoenolpyruvate carboxylase from *Salmonella* by L-aspartate has been described by Maeba & Sanwal (1965). Inhibition of yeast pyruvate carboxylase by L-aspartate has been shown by Palaciañ et al. (1966) and Cazzulo & Stoppani (1968). The present paper describes some additional aspects of the interaction of yeast pyruvate carboxylase with its acyl-CoA activators (acetyl- and palmitoyl-CoA), substrates of the reaction, and the inhibitor, aspartate. In particular, the results indicate that the activation of palmitoyl-CoA follows

† From the Department of Biochemistry, Case Western Reserve University, Cleveland, Ohio 44106. *Received January 19, 1983; revised manuscript received June 24, 1983.* This work was supported in part by National Institutes of Health Grant AM-12245.

* Address correspondence to this author at the Gray Freshwater Biological Institute, Navarre, MN 55392.

[1] Abbreviations: CoA, coenzyme A; DTNB, 5,5′-dithiobis(2-nitrobenzoic acid); TCA, tricarboxylic acid cycle; Tris, tris(hydroxymethyl)aminomethane; $NaDodSO_4$, sodium dodecyl sulfate.

0006-2960/83/0422-5090$01.50/0 © 1983 American Chemical Society